

EXPERIMENTAL STUDY ON CONTACT RELIABILITY OF AUTOMOTIVE ELECTRICAL CONNECTORS

Chen Guoqiang¹, Zhang Pengfei¹, Wang Xin¹, Wang Yanpeng¹, Liu Xuhui¹, Kang Jianli¹

¹School of Mechanical and Power Engineering, Henan Polytechnic University, China

Email: chengq@hpu.edu.cn

Abstract - Contact force is one of the main factors affecting the reliability of the automotive electrical connector. In this paper, a vibration experiment scheme for automotive electrical connectors is proposed to explore the influence of different contact forces on the vibration characteristics of automotive electrical connectors under vibration conditions. A new automotive electrical connector vibration experiment device, including contact force measurement device, vibration experiment device and data acquisition device are built. The relationship between the contact force and the contact resistance of the automotive electrical connector in different vibration environments can be obtained by the experiment. The experimental results show that the vibration experiment device has high reliability and can provide excellent research conditions for the vibration experiment of the automobile electrical connector.

Keywords Automotive electrical connectors, Contact force, Contact resistance, Reliability.

1. Introduction

The electrical connector is an important medium for the automobile electrical module to exchange information, but also the weak link of the automobile electrical module. Due to the harsh environment, the aging of the electrical connector leads to inaccurate transmission signals, which eventually leads to system failure [1,2,3,4,5,6]. In the electrical system, more than half of the failures are caused by components, 40% of which are related to the electrical connector [7,8,9].

Environmental factors not only affect the reliability of the automotive electrical connector, but also greatly affect the service life of the automotive electrical connector. Therefore, some scholars have studied the reliability prediction and fault diagnosis of the automotive electrical connector [10,11,12]. Chen and Li [13] established theoretical equations and reliability models for the temperature-vibration integrated force field, and carried out accelerated life experiments of the automotive electrical connector by orthogonal experiment method [14]. Zhang [15] investigated the degradation process of the automotive electrical connector's contact under vibration force, established a degradation model, carried out experimental verification, and realized a rapid assessment of the reliability of the automotive electrical connector's contact under vibration [16]. Xia [17] established the storage reliability evaluation model of the automobile electrical connector under the combined action of vibration, temperature and insertion and extraction [18]. At the same time, the reliability of the automobile electrical connector was

evaluated by accelerated experiment using experimental data. Luo et al. [19] carried out experiments on the micromotion wear of the automotive electrical connector and predicted the remaining life of the automotive electrical connector under this condition. Chen [20] established a failure model based on the main failure mechanism of the automotive electrical connector, and verified the accuracy of the model through experiments, which can be used for predicting the reliability of the automotive electrical connector. Cao [21] designed an intermittent fault diagnosis system for the automotive electrical connector and established a model with contact resistance and signal transmission as the reliability evaluation index of the automotive electrical connector. Li et al. [22] analysed the mechanism of intermittent faults in the automotive electrical connector, defined the area surrounded by the contact resistance curve and the fault threshold as the generalized severity of intermittent faults, and then integrated the Hidden Semi-Markov Model (HSMM) into the remaining life prediction model for the automotive electrical connector. The validity of the remaining life prediction method based on intermittent failure and HSMM was verified by experiment [23]. Shi et al. [24] proposed a severity assessment method based on Long Short-Term Memory (LSTM) network for accurately assessing the severity of intermittent open-circuit faults, which was effective in evaluating the degree of internal looseness and shock acceleration separately. Li et al. [25] investigated a model and method for predicting the remaining life of the automotive electrical connector based on the

dynamic characteristics of intermittent failure of the automotive electrical connector.

At present, the research on the automotive electrical connector is mainly based on different strategies to establish their failure models and life prediction models, and verify the reliability and residual life through numerical simulation. However, the mechanism of the influence of the vibration parameters and the structure of the reed itself on the minimum contact force of the automobile electrical connector is rarely mentioned. The main purpose of this paper is to obtain the relationship between contact force and contact resistance through experiments. The reliability of automotive electrical connectors is studied.

This paper is organized as follows. Section 2 analyzes the structure of the automotive electrical connector and proposes an experimental scheme. In Section 3, the force loading device, the vibration device, and the data acquisition device are designed. In Section 4, the experiment is carried out and the experimental results are compared with the simulated data to verify the accuracy of the experimental scheme and the reliability of the equipment. Finally, Section 5 summarizes the study.

2. Experimental Scheme

The terminal of the automotive electrical connector used in this experiment is two-piece, as shown in Figure 1. In order to eliminate the influence of initial contact force between terminals, a unilateral reed is used for the experiment. The contact force of the terminal is difficult to measure during the vibration experiment, because the resistance strain gauge cannot be attached to the surface of the female terminal reed. Since the contact resistance between terminals is relatively easy to obtain, the value of the contact force in vibration can be obtained by establishing the relationship between the contact force P and the contact resistance R .

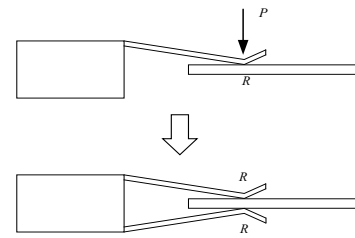


Figure 1: Load schematic diagram of the unilateral reed

The relationship between the total resistance R_z at the contact point and the unilateral reed contact resistance R can be expressed as:

$$R_z = \frac{R}{2} \tag{1}$$

The contact resistance is measured on the terminal under an external load. The relation curve of the contact resistance can be obtained through a series of experimental results. The magnitude and variation of the force can be calculated by measuring the resistance value in the vibration experiment.

The experiment is divided into three steps:

The first step is to apply a constant load to the terminal through a force loading device. A constant current is loaded in the automotive electrical connector through a constant current source. The resistance is calculated by the voltage at both ends of the automotive electrical connection terminal. The voltage measuring device comprises a signal amplifier module, a signal acquisition module and a signal acquisition system. The curve of contact resistance-contact force is obtained through a series of resistance values under different loads.

The second step is to obtain the resistance value during the vibration experiment. The vibration excitation is applied to the automotive electrical connector terminal through the vibration experiment bench. The voltage acquisition system collects voltage. Then the magnitude of the resistance is calculated.

The third step is to calculate the change of contact force during the vibration experiment through the contact resistance-contact force relationship curve and the obtained resistance value. The overall experimental scheme design is shown in Figure 2.

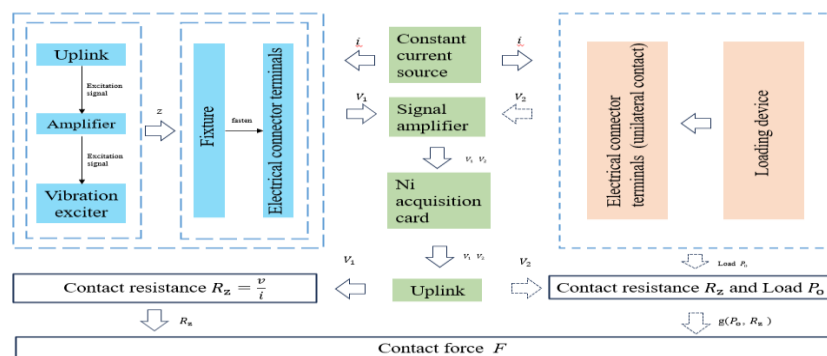


Figure 2: Reliability experimental scheme of the automotive electrical connector

3. Experimental Equipment

3.1 Contact Force Measuring Equipment

In order to obtain the relationship between the contact force and the contact resistance of the automotive electrical connector, a mechanism is designed to fix the automotive electrical connector terminal and apply a stable force as shown in Figure 3. The loading mechanism includes loading, fixing, bearing and force application assemblies. The fixing plate fixes the terminal and the bearing assembly with T-slots adjusts the terminal position. The loading beam can be rotated, the weight is applied to the pressure, and the angle is adjusted with the loading block to ensure complete contact.

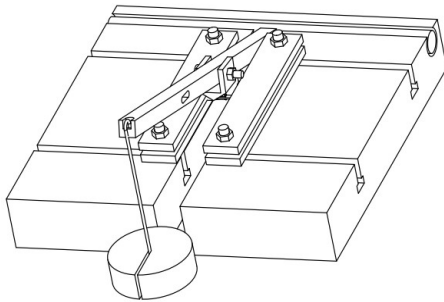


Figure 3: Contact force loading device of the automotive electrical connector

This study proposes a method for determining the circuit turn-on threshold P_i , by adjusting the relative positions between terminals and increasing or decreasing standard weights. Firstly, the reed and the male terminals are brought close to each other but not in contact, then the circuit is changed from broken to open by changing the combination of weights to find the maximum applied load P_{max} and the minimum applied load P_{min} using the dichotomy method. P_i is defined as

$$P_i = \frac{P_{max} + P_{min}}{2} \quad (2)$$

Its error relation to the true critical value P_o is as follows

$$P_o - P_i < \frac{P_{max} - P_{min}}{2} \quad (3)$$

The error of this method is affected by the minimum weight of the weight, and the P_i value varies with the position of the terminal. P_i needs to be subtracted from the final true contact force calculation.

During the experiment, it is critical to ensure that the contact force is loaded vertically. The through-hole is shown in Figure 4. N is the contact line between the loading block and the female terminal reed, line M is parallel to line N and the distance is H . The plane determined by line M and line N is the axisymmetric plane of the loading block, and line M is vertical to the center line L of the through-hole.

The angle between the loading beam and line N is α , the center line K and line M intersect at point P_1 . The first through-hole is set to P_1 . The shape of the hole is a rounded rectangle, and the long side is parallel to the line M to ensure vertical loading. The structure ensures the vertical direction of the force transmit and improves the accuracy of the experiment.

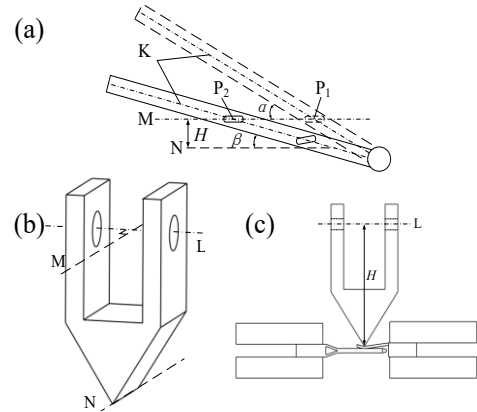


Figure 4: Through-hole positioning method of the loading beam

From the above, it can be seen that the approximate critical load value for the circuit to be switched on is P_i . The total load obtained in the experiment is P_z , then the actual increase in load P_a after the circuit is switched on is as follows

$$P_a = P_z - P_i \quad (4)$$

The load on the terminal needs to be calculated based on the geometry of the structure. The basic structure of the beam is shown in Figure 5.

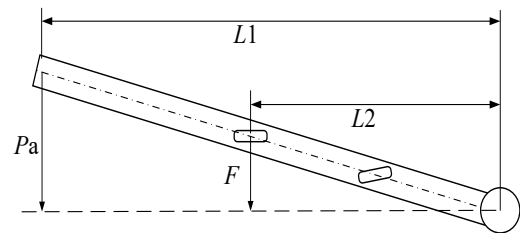


Figure 5: Structure diagram of the loading beam

From Figure 5, the magnitude of the contact force F is calculated as follows

$$F = \frac{L_1}{L_2} P_a \quad (5)$$

where L_1 is the distance from the rotation axis to the end of the loading beam, and L_2 is the distance from the rotation axis to the hole.

3.2 Vibration Equipment

The vibration experiment bench used in this experiment is EDS-300 electric vibration experiment bench, and the experimental equipment is shown in Figure 6.

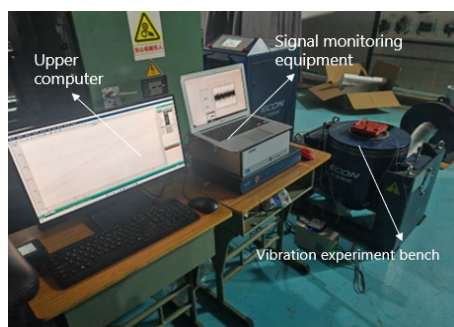


Figure 6: Connection diagram of the experimental equipment

Specialized control software is installed in the upper computer to set the basic parameters and experimental conditions such as vibration amplitude, frequency and time of the vibration experiment bench. The control signal sent by the controller is transmitted to the vibration experiment bench through the power amplifier, where the feedback signal of the acceleration sensor is accepted by the controller to form a closed-loop control system.

The vibration experiment bench comprises a mechanical structure, an elastic support, an electromagnetic actuator, and a control system. When the signal is received, a relative motion occurs between the magnet and the mechanical structure of the electromagnetic driver, and vibrations of different frequencies and amplitudes are generated. The heat sink is used to take away the heat generated by the bench to ensure safety.

The experimental sample should be fixed on the vibration bench. As the automotive electrical connector terminal cannot be fixed directly on the bench, a fixing device is designed. The fixing device is connected to the vibration bench by bolts and the terminal position can be adjusted by T-slots. The fixture was designed with screw holes to allow the use of bolts and nuts for fixing.

The sine vibration module is used in this experiment. Firstly, the sensitivity value of the accelerometer is set before the sensor is fixed. Then the vibration bench parameters such as maximum thrust, acceleration, displacement, and frequency range are set. The frequency range for this experiment is 0-200Hz, and the acceleration and amplitude will be adjusted as needed.

Finally, the schedule is formulated, including frequency selection, vibration duration, and report output options. The experiment is conducted in dwell mode to avoid the effect of long-term vibration on terminal reliability and test result accuracy.

3.3 Data Acquisition Equipment

The data acquisition device is divided into two parts: the hardware and the software. The hardware includes a constant current source, a signal amplifier, a signal acquisition module, and a master computer. The software is a voltage acquisition system based

on LabVIEW. The power supply model used in the experiment is UTP1310+, the output current range is 0-10 mA, and the resolution is 1 mA, which meets the requirements. Due to the small contact resistance, the generated voltage is also small. The signal amplification module AD620 is required to amplify the voltage signal and store the signal into the NI acquisition card. The amplifier can amplify the microvolt voltage, the maximum magnification factor can reach 1000, and the zero point can be adjusted by the zeroing potentiometer.

The signal conditioning module outputs analog signals, and digital signals need to be collected and processed. Therefore, an acquisition module is needed to convert analog signals into digital signals. The selected data acquisition card model is NI USB-6002. The single-ended channel is 8, the differential channel is 4, the resolution of ADC and DAC is 16 bits, and the maximum sampling rate is 50kS/s, which meets the data acquisition requirements.

The purpose of the experiment is to collect voltage signals. The program includes acquisition module, storage module, and visualization module. In the acquisition module, a channel is created to collect the voltage signal. The physical channel must correspond to the interface of the NI acquisition card. The maximum voltage and the minimum voltage are the range of the NI acquisition card. The output range of the NI USB-6002 is $\pm 10V$. The terminal configuration is mainly single-ended mode and differential mode. Since the master computer is a laptop, which belongs to the floating source, while the constant current source is a three-wire power supply, which belongs to the ground source, the wiring method should choose the ground reference single-ended mode. The sampling clock controls the rate of collecting or generating samples. The sampling mode includes limited sampling, continuous sampling, hardware timing single point sampling, etc. Continuous sampling is selected in this experiment. The sampling rate determines the speed at which the data is collected and placed in the hardware buffer. The number of samples per channel determines the number of data from the hardware buffer to the software buffer. Generally, the number of samples per channel is set to one-tenth of the sampling rate. The sampling clock source of this experiment is selected internally.

4. Experiment

4.1 Contact Resistance Experiment

According to QC _ T 1067.1-2017, when the terminal contact resistance experiment is carried out, the current is not more than 200 mA, so 100 mA is used. Due to the low resistance of the terminal, the voltage generated is small, and the signal amplifier is needed to amplify. The preset amplification is 100 times, and the actual is 108.84 times. The experimental data is shown in Table 1.

Table 1. Experimental data of the contact force-contact resistance

Load/g	Voltage /V					Average/V	Resistance/mΩ
	1	2	3	4	5		
100	0.06739	0.06875	0.07026	0.06953	0.06855	0.06890	6.330
500	0.03906	0.03686	0.03868	0.03855	0.03803	0.03824	3.513
1000	0.03385	0.0339	0.03434	0.03452	0.03353	0.03403	3.126
1500	0.03294	0.03195	0.02738	0.02931	0.02728	0.02977	2.735

Table 1 shows that four groups of loads are designed, and each group of loads is tested five times. The average value of the contact voltage of the five groups of experiments is calculated to reduce the experimental error. The resistance value decreases with increasing load, and the rate of decrease gradually slows down. According to the empirical equation, the relationship between the contact resistance R and the contact force F is expressed as follows

$$R = \frac{K}{(0.102F)^M} \tag{6}$$

where K and M are unknown coefficients.

Due to the great influence of different terminals or states on the resistance, the error of the direct estimation coefficient is large. Therefore, the contact force-contact resistance model is established by using the experimental data to obtain a more accurate relationship curve. The fitting curve is shown in Figure 7.

Taking Equation (6) as the model equation, the relationship between the contact force and the contact resistance obtained by fitting is as follows:

$$R = \frac{2.93462}{(0.102F)^{0.31117}} \tag{7}$$

The goodness of fit is 0.953. The result shows that the model has a high matching degree with the data. The resistance value can be calculated according to the contact force value. The resistance of the bilateral reed is greater than half of the unilateral reed. The simulated data shows that the contact force at rest is 10.532 N, which can be simulated by 1075 g weight. The results are shown in Table 2.

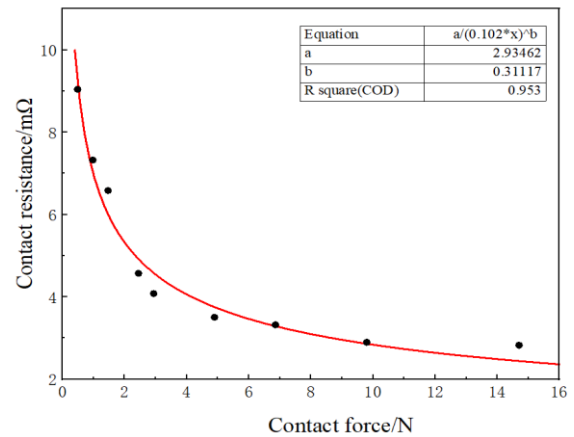


Figure 7: Fitting curve of the contact force - contact resistance

Table 2. Comparison of the resistance between unilateral and bilateral reeds

Group	1	2	3	4	5
Unilateral resistance /mΩ	2.816	3.035	2.952	2.856	2.889
Bilateral resistance /mΩ	2.119	2.216	2.104	2.056	2.179
Ratio	75.20%	73.01%	71.27%	71.99%	75.42%

From Table 2, it can be seen that the bilateral resistance accounts for about 70 % ~ 75 % of the unilateral resistance, and the average value of the five groups of experiments is 73.39 %, which is used as the converted coefficient of the unilateral and bilateral resistance. Substituting the contact force of the bilateral reed 10.532 N into the model, the unilateral contact resistance is 2.8631 mΩ, and the bilateral contact resistance is 2.1012 mΩ. The measured contact resistance of the automotive

electrical connector is 2.219 mΩ, and the error with the model value is 5.31 %, which proves that the model effectively and describes the relationship between the contact force - contact resistance.

4.2 Vibration Experiment

The vibration experiment is carried out using the vibration experiment bench, and the value of the contact resistance is collected by the bench. Two

groups of experiments are carried out, which are different in the terminal fixation method: one is to fix a single terminal and wire, as shown in Figure 8 (a),

and the other is that two terminals were fixed to the clamping device, as shown in Figure 8 (b).

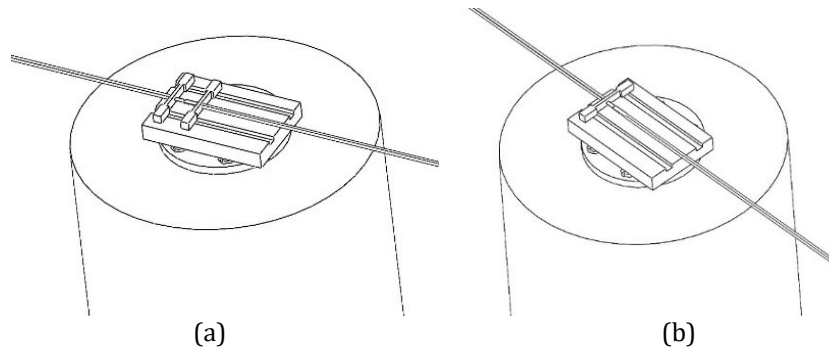


Figure 8: Two fixing methods of the terminal in vibration experiment

Four groups of vibration amplitudes are designed in the experiment, and each group of vibration amplitudes corresponds to four groups of different frequencies, a total of 16 vibration conditions. In order to improve the reliability of the results, two experiments are carried out for each vibration condition, and the specific vibration conditions are shown in Table 3.

Table 3. Vibration conditions for fixing a single terminal

	1	2	3	4
Amplification/mm	0.50	0.75	1.00	1.50
Frequency /Hz	50	75	100	150

After fixing the clamping device, the terminal is connected to the circuit, and the data collector is connected to the computer. The acquisition system is opened, the physical channel is selected as Dev1 / A10, and the wiring is set to RSE. According to the Nyquist theorem, the sampling rate is set to 1000Hz.

The vibration conditions are set in the control software, and the experiment is initiated. The collected data is the amplified voltage value, as shown in Figure 9.

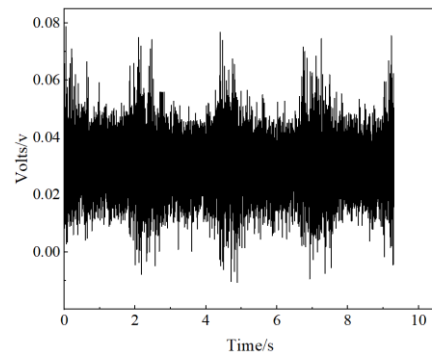


Figure 9: Voltage data with amplitude of 1.5 mm and frequency of 100 Hz

The above signals are converted from the time domain to the frequency domain by fast Fourier transform as shown in Figure 10.

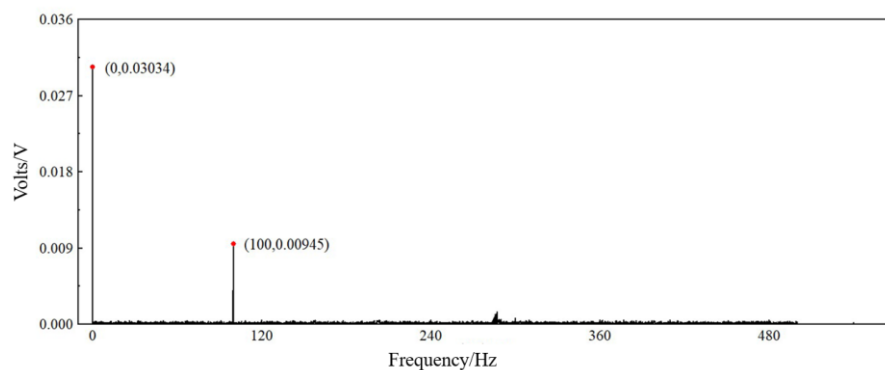


Figure 10: Fast Fourier transform results of voltage data with amplitude of 1.5mm and frequency of 100Hz.

From Figure 10, the signal is mainly composed of DC and 100Hz AC components. The expression is as follows:

$$V = 0.03034 + 0.00945 \sin (200\pi t) \quad (8)$$

where V is the voltage.

The maximum contact resistance is 3.914 mΩ. The results of different experimental groups are obtained by the same method, as shown in Table 4.

Table 4. Contact resistance of the vibration experiment of fixing a single terminal

Amplification/mm	Frequency/Hz	Groups	Contact resistance/mΩ	Average/mΩ
0.50	50	1	2.467	2.469
		2	2.471	
	75	1	2.581	2.580
		2	2.578	
	100	1	2.720	2.721
		2	2.721	
	150	1	3.155	3.154
		2	3.153	
0.75	50	1	2.486	2.486
		2	2.486	
	75	1	2.649	2.648
		2	2.646	
	100	1	2.993	2.989
		2	2.985	
	150	1	25.364	23.276
		2	21.188	
1.00	50	1	2.512	2.508
		2	2.503	
	75	1	2.901	2.899
		2	2.897	
	100	1	3.468	3.470
		2	3.472	
	150	1	37.856	41.200
		2	44.544	
1.50	50	1	2.525	2.526
		2	2.527	
	75	1	3.610	3.613
		2	3.616	
	100	1	3.914	3.915
		2	3.915	

From Table 4, When the vibration amplitude is the same, the contact resistance increases with the increase of the vibration frequency. When the vibration frequency is the same, the contact resistance increases with the increase of the vibration amplitude. The average value of the two tests is taken as the contact resistance value of the group, and Figure 11 is drawn with frequency and amplitude as abscissa respectively. Figure 11 (a) shows that at 150 Hz, 0.75 mm and 1 mm

amplitudes, the contact resistance far exceeds the reliability requirement, the connector has failed, and there is no need to try the 1.5 mm amplitude again. Figure 11 (b) shows the change of the contact resistance when the frequency is the same and the amplitude is different.

When the vibration frequency is 150 Hz, the growth rate of the contact resistance increases significantly.

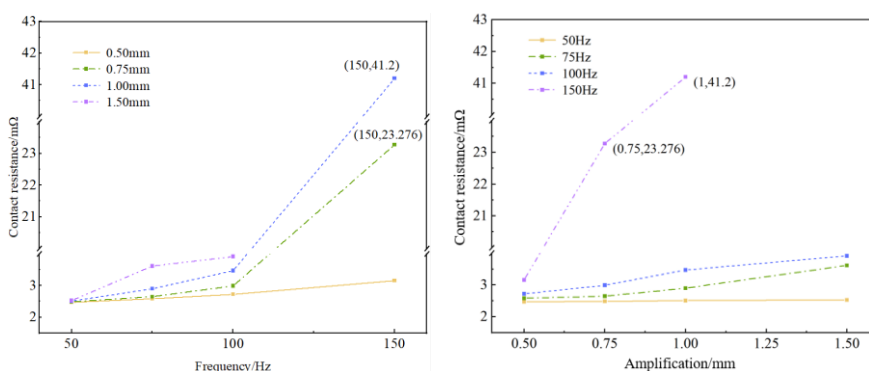


Figure 11: Change rule of the contact resistance of fixing a single terminal

Because only a single terminal is fixed during the experiment, the two terminals have a large relative displacement when the vibration amplitude and vibration frequency are large.

At this time, the friction force will be reduced, which will cause the terminal to fall off. Therefore, the experiment of fixing two terminals is carried out, and the vibration conditions are adjusted as shown in Table 5.

Table 5. Vibration conditions of fixing two terminals

	1	2	3	4
Amplification/mm	0.50	0.75	1.00	1.50
Frequency/Hz	50	75	100	150

The processing method of the experimental data is the same as that of the previous group. The signal is processed by fast Fourier transform, and the results are shown in Table 6.

Table 6. Contact resistance of the vibration experiment of fixing two terminals

Amplification/mm	Frequency/Hz	Groups	Contact resistance/mΩ	Average/mΩ
0.5	50	1	2.274	2.276
		2	2.278	
	100	1	2.410	2.396
		2	2.382	
	125	1	2.468	2.470
		2	2.471	
	150	1	2.798	2.800
		2	2.802	
1.0	50	1	2.318	2.316
		2	2.314	
	100	1	2.603	2.601
		2	2.599	
	125	1	2.842	2.839
		2	2.836	
	150	1	3.077	3.088
		2	3.099	
1.5	50	1	2.374	2.373
		2	2.371	
	100	1	2.800	2.796
		2	2.792	
	125	1	2.989	2.989
		2	2.988	
	150	1	3.510	3.506
		2	3.502	

From Table 6, the changing trend of the contact resistance at the same amplitude and different frequencies and the same frequency and different amplitudes is the same as the results of fixing a

single terminal. Figure 12 shows the changing trend of the contact resistance with frequency and amplitude.

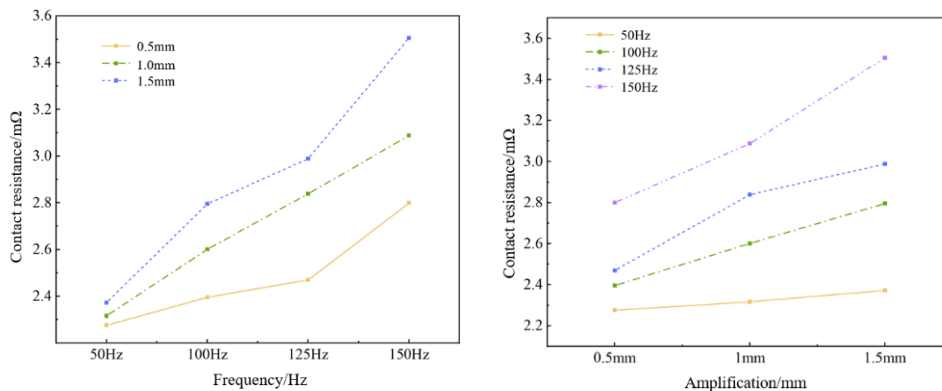


Figure 12: Change rule of the contact resistance of fixing two terminals

From Figure 12, the contact resistance increases with the increase of vibration amplitude and frequency, but there is no sharp increase. The results of the two experiments are shown in Figure 13.

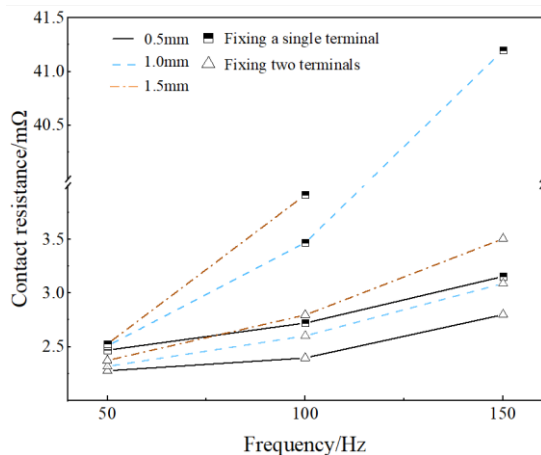


Figure 13: Comparison of the experimental result of different fixing methods

From Figure 13, under the same experimental conditions, the stability of fixing two terminals is better than that of fixing a terminal.

The simulated results of the second fixing mode and the vibration frequency of 50 Hz are selected. The contact force obtained by the simulation is converted into the change of the contact resistance through the relationship curve of the contact force-contact resistance, and compared with the experimental results. The results of the comparison are shown in Figure 14.

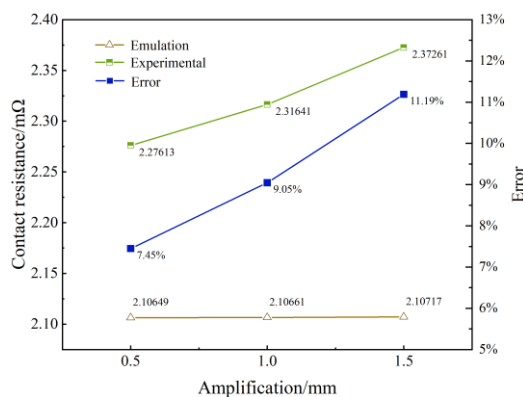


Figure 14: Comparison of the contact resistance of experiment and simulation

From Figure 14, there is a certain error between the simulated results and the experimental results, but the overall trend is consistent.

5. Conclusions

This study investigates the effect of vibration on the reliability of the automotive electrical connector.

- An experimental scheme comprising both hardware and software is designed.

- The relationship between the contact force and the contact resistance and the change of the contact resistance in a vibrating environment are investigated.

- The relationship curves are obtained by fitting the experimental data, and the changes of the contact resistance under different fixation methods and vibration conditions are compared.

It has been found that vibration has a significant effect on the reliability of the automotive electrical connector, which may lead to an increase in contact resistance or even failure. Although it provides a reference for the design of the electrical connector, the study is mainly limited to sinusoidal vibration excitation and does not involve random or shock vibration situations. This experiment mainly studies the reliability of the automotive electrical connector under sinusoidal vibration excitation. In actual use, it may be subjected to random vibration or impact vibration, which needs further analysis and research. In the study, a single electrical connector terminal is taken as the research object, and a wire harness plug can be established in the future.

Acknowledgments

The work is supported by the Key Technologies R&D Program of Henan Province (No.222102220024). The authors would like to thank the anonymous reviewers for their constructive feedback.

References

- [1] Chen, P. and He, F. (2022). Analysis and Research on Failure Mode and Failure Mechanism of Automobile Electrical Connector, *Electronic Product Reliability and Environmental Testing*, Vol. 40, No. 5, pp.100-105.
- [2] Han, Y., Meng, Y., Zhang, C. and Ren, W. (2024). Experimental Investigation of Mechanical Wear Failure Mechanism for Connectors, *Electrical and Energy Efficiency Management Technology*, No. 3, p.60-65.
- [3] Ji, R., Gao, J., Flowers, G. T., Xie, G., Cheng, Z. and Jin, Q. (2017). The Effect of Electrical Connector Degradation on High-frequency Signal Transmission, *IEEE Transactions on Components, Packaging and Manufacturing Technology*, Vol. 7, No. 7, pp.1163-1172.
- [4] Liu, X., Hu, S., Xiao, Q., Deng, G., Zheng, Y., Gao, M., Zhang, D., Cao, H., Wang, Z., Chen, D. and Yang, W. (2024). An Investigation of The Electrical Contact Failure of JPT Electric Connectors Used in Automobiles Under Multiple Stresses, *Wear*, Vol. 552-553, p.205458.
- [5] Thukral, V., Roucou, R., Chou, C., Zaal, J. J. M., van Soestbergen, M., Rongen, R. T. H., van Driel, W. D. and Zhang, G. Q. (2024). Understanding Board Level Vibrations in Automotive Electronic Modules, *Microelectronics Reliability*, Vol. 159, p.115430.

- [6] Wei, Z., and Liu, C. (2022). Characteristics and Causes of Typical Failure Modes of Electrical Connectors, *Failure Analysis and Prevention*, Vol. 17, No. 1, p.63-72.
- [7] Czerlunczakiewicz, E., Majerczak, M. and Bonato, M. (2024). Fatigue Simulations for Automotive Components undergoing Vibration Loadings: Effect of Nonlinear Behavior, *Procedia Structural Integrity*, Vol. 57, pp.743-753.
- [8] Guo, J. (2021). Typical Failure Analysis Example of Electric Connector, *Environmental Technology*, Vol.39, No. 2, pp.145-149.
- [9] Li, Q., Li, J., Chen, X., Li, N., She, Z. and Wang, L. (2021). The Overview and Research Status Analysis of Electrical Connectors, *Environmental Technology*, No. 6, pp115-119.
- [10] Liu, Y., Jia, Y., Yang, J., Song, S., Wu, B. and Li, J. (2018). Research of Mechanical State Diagnosis Techniques in GIS Bus Connector Based on Mechanical Vibration, *2018 12th International Conference on the Properties and Applications of Dielectric Materials (ICPADM)*, Xi'an, China, 2018, pp.682-685.
- [11] Lin, W. C. and Du, X. (2018). Prognosis of Power Connector Disconnect and High Resistance Faults, *2018 IEEE International Conference on Prognostics and Health Management (ICPHM)*, Seattle, WA, USA, 2018, pp.1-8.
- [12] Qian, P., Wang, Y., Chen, W., Wang, Z. and Wei, Y. (2023). Contact Reliability Design Modeling for Wire Spring-hole Electrical Connectors, *Microelectronics Reliability*, Vol. 148, p.115182.
- [13] Chen, P. and Li, Q. (2022). Research on Accelerated Life Evaluation Method of Automotive Electrical Connector, *Electronic Product Reliability and Environmental Testing*, Vol. 40, No. 6, p14-19.
- [14] Zhang H., Li X. and Zhou Y. (2023). Thermal failure analysis of special-shaped crown spring connectors for rail vehicles, *Engineering Failure Analysis*, Vol. 149, p.107241.
- [15] Zhang, W. (2020). *Study on Step-stress Acceleration Degradation Test of Electrical Connector Contacts under Vibration*. Master's thesis, Zhejiang Sci-Tech University, Hangzhou, China.
- [16] Abbasi A., Nazari F. and Nataraj C. (2022). Adaptive modeling of vibrations and structural fatigue for analyzing crack propagation in a rotating system, *Journal of Sound and Vibration*, Vol. 541, P.117276.
- [17] Xia, H. (2019). *Research on Combined Stresses Accelerated Life Test and Statistical Analysis of Electrical Connector*. Master's thesis, Zhejiang Sci-Tech University, Hangzhou, China.
- [18] Montes R.O.P., Silva F.M.A. and Pedroso L. J. (2024). Free vibration analysis of a clamped cylindrical shell with internal and external fluid interaction, *Journal of Fluids and Structures*, Vol. 125, p.104079.
- [19] Luo, Y., Liu, T., Zhang, Z. and Wu, X. (2022). Performance Degradation Law and Life Prediction of Electrical Connector Contacts, *Journal of Ordnance Equipment Engineering*, Vol. 43, No. 9, p.39-47.
- [20] Chen, P. (2020). *Experimental analysis of reliability of automotive electrical connectors*. Master's thesis, Xidian University, Xian, China.
- [21] Cao, S. (2021). *Design and Implementation of Intermittent Fault Diagnosis System for Electrical Connectors in Vibration Environment*. Master's thesis, Chongqing University, Chongqing, China.
- [22] Li, Q., Lyu, K., Qiu, J., and Liu, G. (2019). Research on Intermittent Failure Re-presentation of Electrical Connector Based on Accelerated Test, *Proceedings of the Institution of Mechanical Engineers, Part O: Journal of Risk and Reliability*, Vol. 233, No. 3, p317-327.
- [23] Li, H., Lv, K., Shen, Q., Qiu, J. and Liu, G. (2018). Method of Electrical Connector Intermittent Fault Reproduction, *Aircraft Engineering and Aerospace Technology*, Vol. 90, No. 6, p946-955.
- [24] Shi, J., He, Q. and Wang, Z. (2021). An LSTM-based Severity Evaluation Method for Intermittent Open Faults of An Electrical Connector Under A Shock Test, *Measurement*, Vol. 173, p.108653.
- [25] Li, Q., Lv, K., Qiu, J. and Liu, G. (2018). Research on Residual Life Prediction for Electrical Connectors Based on Intermittent Failure and Hidden Semi-Markov Model, *Applied Sciences*, Vol. 8, No. 8, p1373.